Spectra of turbulent fluctuations of Euler angles of unmanned aerial vehicles in the altitude holding mode

Alexander P. Shelekhov[a*], Aleksey L. Afanasiev[b], Alexey A. Kobzev[a], Olga S. Chupina[a], Alexey E. Tel'minov[a], Evgenia A. Shelekhova[a]

[a]Institute of Monitoring of Climatic and Ecological Systems SB RAS, 10/3, Academichesky Ave, 634055, Tomsk, [b]V.E. Zuev Institute of Atmospheric Optics Organization SB RAS, 634055, Tomsk, Russia, 1, Academician Zuev square

ABSTRACT

The turbulent power spectra of Euler angles are studied. The results of their comparison with the spectra of turbulent fluctuations of wind velocity components in the atmosphere are present. Equations are derived for estimating the horizontal wind components as a function of the means and fluctuation components of Euler angles. Time series of turbulent fluctuations in pitch, roll, and yaw angles, as well as time series of turbulent fluctuations of wind velocity components are obtained during an experiment, which was carried out at Geophysical Observatory of IMCES SB RAS in Tomsk Akademgorodok (Russia). The time series of Euler angles and wind speeds were recorded with a frequency of 10 Hz. The automated weather station data witness anisotropy of turbulent flow speed fluctuations during the measurements in the atmosphere: the spectra of fluctuations of the horizontal components coincide, but differ from the spectrum of vertical fluctuations. The fluctuations of the Euler angles show similar behavior: the spectra of fluctuations of pitch and roll angles coincide, but differ from the spectrum of fluctuations of the yaw angle. The spectra of fluctuations of pitch and roll angles and the spectra of fluctuations of the horizontal wind velocity components generally coincide, though differences are observed in the high-frequency region of the spectrum. In contrast to fluctuations of pitch and roll angles, the spectrum of fluctuations of the yaw angle coincides with the spectrum of the vertical wind velocity component in the high-frequency region.

Keywords: atmosphere, turbulence, UAVs, spectrum, fluctuations, Euler angles, wind velocity components, altitude holding mode.

1. INTRODUCTION

Atmospheric turbulence is a key factor which reduces potential capabilities of different systems. One the main ways to acquire reliable information about atmospheric turbulence is the use of unmanned aerial vehicles (UAVs), which have certain advantages as compared, for example, to sensors attached to a tethered balloon. UAVs become an indispensable tool in atmospheric monitoring in urban environment, forests, canyons, and other areas with complex relief. As a result, techniques based on the use of UAVs are of great interest for solution of a wide range of scientific and applied problems, such as: air pollution monitoring, urban atmosphere and local climatic zones, urban climate under conditions of global the climate change, etc.

Some problems associated with the atmospheric turbulence effect on UAV operation are described in [1]. The analysis [2] showed multirotor UAV to be more promising in low-altitude remote sounding than tethered balloons with sensors, since the former are inexpensive, easy to operate, long-run in a wide range of atmospheric conditions, and reusable. The advantages of multirotor UAVs include vertical take-off and landing and a possibility of hovering at a fixed point. These advantages make this UAV type an ideal platform for vertical profiling or contact derivation of time variations in the atmosphere.

The wind speed and direction were measured in [2] by direct and indirect methods. Within the direct 2D method, an acoustic anemometer was mounted on a hexorotor with a large carrying capacity; in the indirect method, wind speed and direction were found based on pitch and roll angles. The data on the angles were recorded with a frequency of 10 Hz, and data on the wind speed and direction were recorded with a frequency of 1 Hz by anemometers fixed at three 10-meter

* ash@imces.ru

towers on the experimental site. The studies have shown that direct and indirect methods allow quite accurate estimation of the wind speed, while the wind direction is more accurately estimated by an indirect approach. An indirect approach was suggested in [3], but it was tested in a wind tunnel, but not in situ, like in [2].

Works [4, 5] are devoted to the development of a model approach to vertical profiling of horizontal components of the wind velocity with the use of a quadcopter in the hover mode and in vertical flight. The approach suggested to measuring horizontal wind was tested using two sodars and an acoustic anemometer. The time resolution of the sodars used was 30 and 300 s, and of the acoustic anemometer 1 s. In general, data from [3, 4] proves the efficiency of the approach in vertical wind profiling with the use of a quadcopter in the lower atmosphere.

The wind velocity estimate in a turbulent atmosphere with the help of small UAVs without a wind sensor and the machine learning approach are studied in [6]. The Dryden model and the LES model of the atmospheric boundary layer are used in numerical calculations. The simulation results show a neural network with long short-term memory to provide for better estimates of wind speed than linear approaches, especially in the presence of strong turbulence.

This work is aimed at the study of turbulent power spectra of Euler angles of a quadcopter and their comparison with the spectra of turbulent fluctuations of the wind velocity components in the atmosphere. We derive equations for the horizontal wind components as functions of the means and fluctuation components of the Euler angles under perfect quadcopter hovering. The basic equations of the theory of turbulence necessary for the correct comparison between the theory and experiment are given. General information about the experiment is presented; the measurement results obtained with the use of a DJI Phantom 4 Pro quadcopter and the AMK-03 automatic weather station are analyzed. The power spectra of the Euler angles of a quadcopter and the spectra of turbulent fluctuations of the wind velocity components are compared.

2. WIND VELOCITY ESTIMATION

Dynamic equations for the center of gravity of a quadcopter can be written in an inertial coordinates associated with the Earth as

$$\ddot{x} = \left(s_\varphi s_\psi + c_\varphi s_\theta c_\psi\right)\frac{T}{m} + \frac{F_x}{m}, \tag{1}$$

$$\ddot{y} = \left(-s_\varphi c_\psi + c_\varphi s_\theta s_\psi\right)\frac{T}{m} + \frac{F_y}{m}, \tag{2}$$

$$\ddot{z} = c_\varphi c_\theta \frac{T}{m} - g + \frac{F_z}{m}, \tag{3}$$

where $s_{(\bullet)} = \sin(\bullet)$, $c_{(\bullet)} = \cos(\bullet)$; φ is the roll angle; θ is the pitch angle; ψ is the yaw angle; T is the aerodynamic force generated by propellers; F_x, F_y, and F_z are the drag force components along the *x*, *y*, and *z* axes; m is the quadcopter mass; g is the gravity acceleration.

The components of the drag force along the *x*, *y*, and *z* axes, which arise during a quadcopter flight have the form:

$$F_j = -c_j\left(v_j - w_j\right) \tag{4}$$

in the linear case and

$$F_j = -\frac{1}{2}\rho C_j A_j \operatorname{sgn}\left(v_j - w_j\right) \times \left(v_j - w_j\right)^2 \tag{5}$$

in the square-law case. In Eqs. (4) and (5), c_j and C_j are the drag indices along the *x*, *y*, and *z* axes; j is the subscript for enumeration of the orthogonal components of vectors, i.e., $j \in \{x, y, z\}$; v_j are the quadcopter velocity components, and w_j are the velocity components of a turbulent flow in the atmosphere ; ρ is the air density; A_j are the projections of the quadcopter area on the corresponding axes; $\operatorname{sgn}(\bullet)$ is the sign function.

Let us consider the case of perfect hovering, which takes place when all the forces acting on the quadcopter are compensated and $v_j = 0$. After necessary transformations, the equations for estimation of horizontal components of the turbulent flow velocity in the approximation of small pitch and roll angles and for $\psi \approx 0$ take the form

$$\hat{w}_x = -\frac{mg}{c_x}\left(\langle\theta\rangle + \theta'\right), \tag{6}$$

$$\hat{w}_y = \frac{mg}{c_y}\left(\langle\varphi\rangle + \varphi'\right) \tag{7}$$

in the linear case and

$$w_x = -\operatorname{sgn}\left(\langle\theta\rangle\right)\sqrt{\frac{2mg}{\rho C_x A_x}|\langle\theta\rangle|}\left\{1+\operatorname{sgn}\left(\langle\theta\rangle\right)\frac{\theta'}{2|\langle\theta\rangle|}\right\}, \tag{8}$$

$$w_y = \operatorname{sgn}\left(\langle\varphi\rangle\right)\sqrt{\frac{2mg}{\rho C_y A_y}|\langle\varphi\rangle|}\left(1+\operatorname{sgn}\left(\langle\varphi\rangle\right)\frac{\varphi'}{2\langle\varphi\rangle}\right) \tag{9}$$

in the square-law case. Equations (6) – (9) imply that the estimates of the horizontal components of turbulent flow velocity are the sum of the regular and fluctuation parts regardless of the drag model. The regular part of the estimates is determined by the average values of the $\langle\varphi\rangle$ and $\langle\theta\rangle$ angles, and the fluctuation part is proportional to the fluctuations of the roll and pitch angles. Thus, Equations (6) – (9) allows the comparison between the relative spectra of horizontal wind velocity fluctuations and of fluctuations of the roll and pitch angles.

3. MODEL OF ATMOSPHERIC TURBULENCE

To characterize the field of turbulent flow velocity in the atmosphere $\mathbf{w}(\mathbf{r})$, we introduce the notions of the average velocity $\langle\mathbf{w}\rangle = \{\langle w_X\rangle, \langle w_Y\rangle, \langle w_Z\rangle\}$, the fluctuation velocity $\mathbf{w}' = \{w_X', w_Y', w_Z'\}$, and the correlation function of fluctuations of the turbulent flow velocity $B_{pq}(\mathbf{r}-\mathbf{r}') = \langle w_p'(\mathbf{r}) w_q'(\mathbf{r}')\rangle$ [7, 8]:

$$\mathbf{w}(\mathbf{r}) = \langle\mathbf{w}(\mathbf{r})\rangle + \mathbf{w}'(\mathbf{r}), \tag{10}$$

$$B_{pq}(\mathbf{r}-\mathbf{r}') = \langle w_p'(\mathbf{r}) w_q'(\mathbf{r}')\rangle, \tag{11}$$

where $\langle\ldots\rangle$ is the statistical averaging operator; the subscripts p and q designate the orthogonal components of the vector $\mathbf{w}'(\mathbf{r})$ along the X, Y, and Z axes in the coordinates accepted in meteorology [7].

Let us assume [8] the 3D spatial spectrum of wind velocity fluctuations to be a second-order tensor. Then, the spectral tensor $\Phi_{ij}(k)$ for isotropic fluctuations $\mathbf{w}'(\mathbf{r})$ is defined by a scalar function of the wavenumber $k = |\mathbf{k}|$:

$$\Phi_{ij}(k) = \frac{1}{4\pi k^2}\left(\delta_{ij} - \frac{k_i k_j}{k^2}\right)E(k), \tag{8}$$

where $E(k)$ is the energy spectrum of wind velocity fluctuations; k_i are the coordinates of the vector $\mathbf{k}$, δ_{ij} is the Kronecker's delta.

In the case of isotropic fluctuations of the turbulent flow velocity, the Kolmogorov–Obukhov five-thirds law [8] is fulfilled in the inertial range of wavenumbers:

$$E(k) \sim \varepsilon \cdot k^{-5/3}, \tag{9}$$

where ε is the dissipation rate of the turbulence kinetic energy.

4. MEASUREMENT RESULTS

Experiments were carried out on the basis of the Geophysical Observatory of IMCES SB RAS, located in Tomsk Akademgorodok (Russia) on February 20, 2020. It started at 10:21 UTC and ended at 10:34 UTC. Figure 1 shows the flight path of the quadcopter during the experiment. The starting point of the DJI Phantom 4 Pro quadcopter was in close proximity to the foundation of the observatory building. After takeoff, the UAV rose to an altitude of 28 m and flew up to the AMK-03 automated weather station fixed on a mast mounted on the observatory roof; the axis of the quadcopter was northward oriented. The quadcopter held the altitude for about 10 min near AMK-03 and then returned to the starting point.

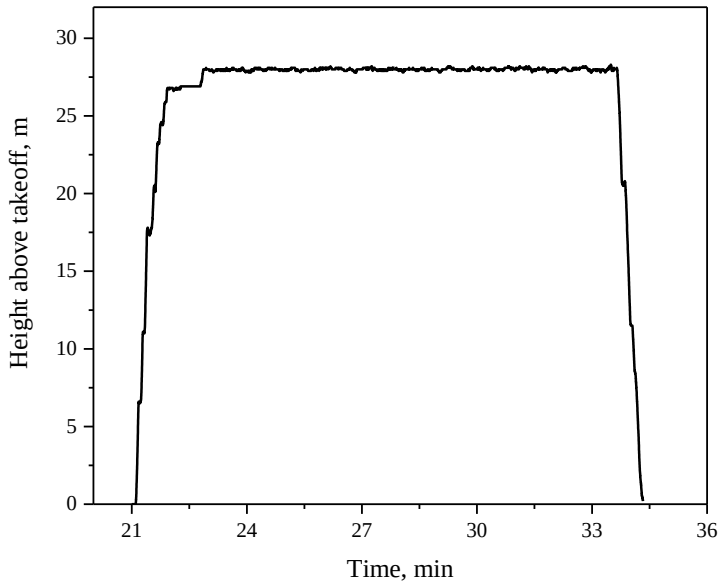

Figure 1. Quadcopter flight trajectory during the experiment.

AMK-03 automated weather station has been designed to measure and record wind speed and direction, air temperature and relative humidity, and atmospheric pressure. The wind data were recorded at a frequency of 10 Hz; the quadcopter status was recorded with the same frequency, that is, time series of roll, pitch, and yaw angles.

According to the Tomsk International Airport, which is located ~10 km from the building of the Geophysical Observatory of IMCES SB RAS, poor weather conditions were observed during the experiment in terms of quadcopter flight: south-south-west wind with a speed of 6.0 m/s, air temperature of –1.5°C, 100% air humidity, and snowing.

Variations in the quadcopter velocity components along the *x*, *y*, and *z* axes during hovering are shown in Fig. 2. These components are generally zero during the measurements, though there are short time periods when the forces which act the UAV exceed the capabilities of the control system and high-precision positioning is violated. After restoration of the control, the quadcopter begins moving to its initial position and stops upon reaching it. Thus, the periods when the quadcopter positioning is violated can be ignored due to their insignificance, and the hovering between 10:23:00 and 10:33:00 UTC can be considered perfect.

Let us consider the behavior of pitch, roll, and yaw angles in a turbulent atmosphere in the altitude holding mode. The average pitch, roll, and yaw angles and the average horizontal flow velocity components are $\langle\theta\rangle$=3.8°, $\langle\varphi\rangle$=–1.7°, $\langle\psi\rangle$=1.4°, $\langle w_Y\rangle$=-2.7 m/s, and $\langle w_X\rangle$=-1.1 m/s. Figure 3 shows the time series of fluctuations of the pitch, roll, and yaw angles (black curves), as well as fluctuations of the horizontal wind components w'_Y and w'_X (red curves) measured by the AMK-03 automated weather station. One can see that the fluctuations of the pitch and yaw angles generally coincide

with the fluctuations of the horizontal wind components, and the differences are observed in the high-frequency fluctuation region.

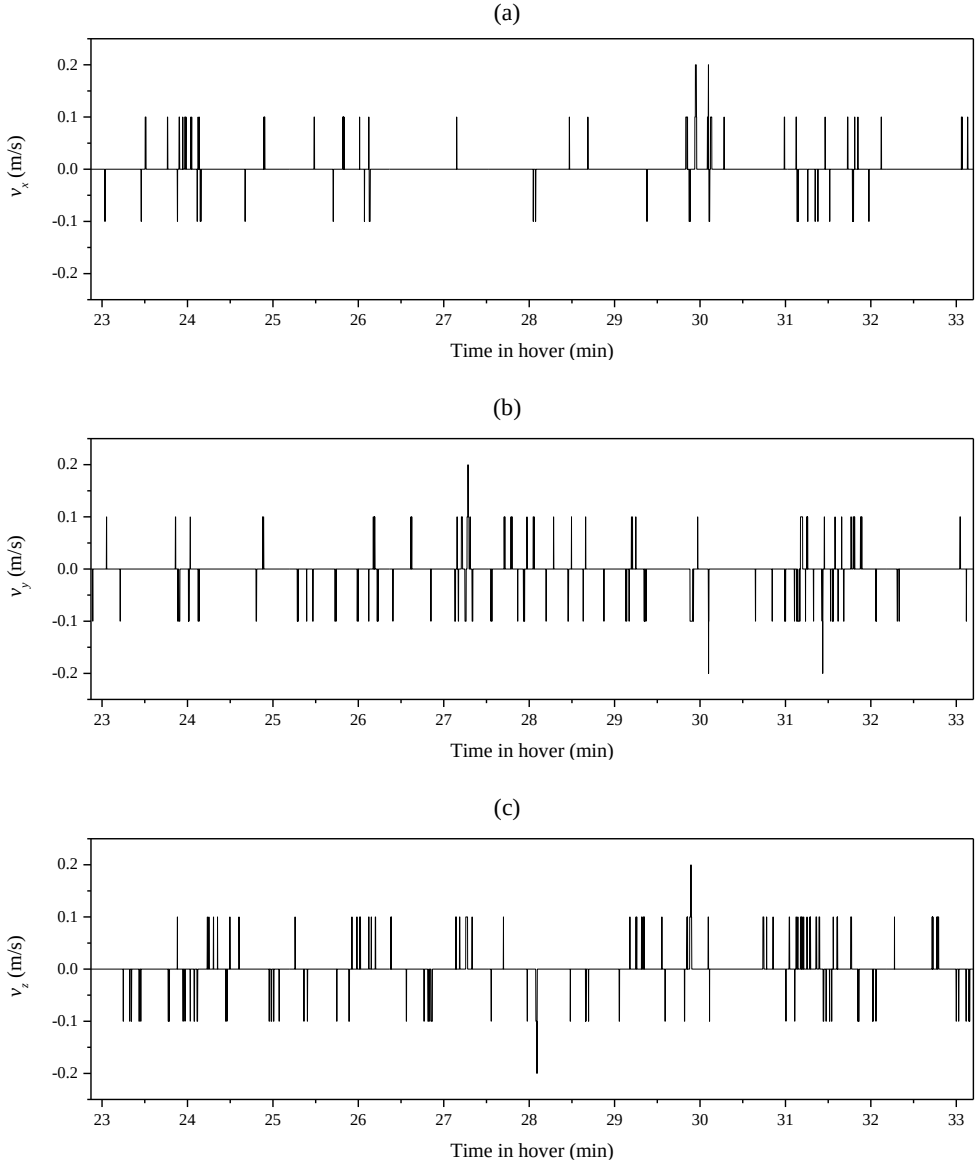

Figure 2. Quadcopter velocity components along the (a) *x*, (b) *y*, and (c) *z* axes during hovering.

To objectively estimate the power spectra of fluctuations of the roll, pitch, and yaw angles and the wind velocity components in a turbulent atmosphere, we used the 10-minute averaging. The power spectra were calculated using standard FFT algorithms with a smoothing procedure.

Figure 4 shows the relative power spectra of fluctuations of the turbulent flow velocity calculated on the basis of AMK-03 data, as well as the relative power spectra of the fluctuations of the pitch, roll, and yaw angles calculated on the basis of the DJI Phantom 4 Pro quadcopter telemetry data. The dashed curve in Figure 4 shows the power spectrum of fluctuations which corresponds to the Kolmogorov–Obukhov five-thirds law, and σ^2 is the normalization coefficient.

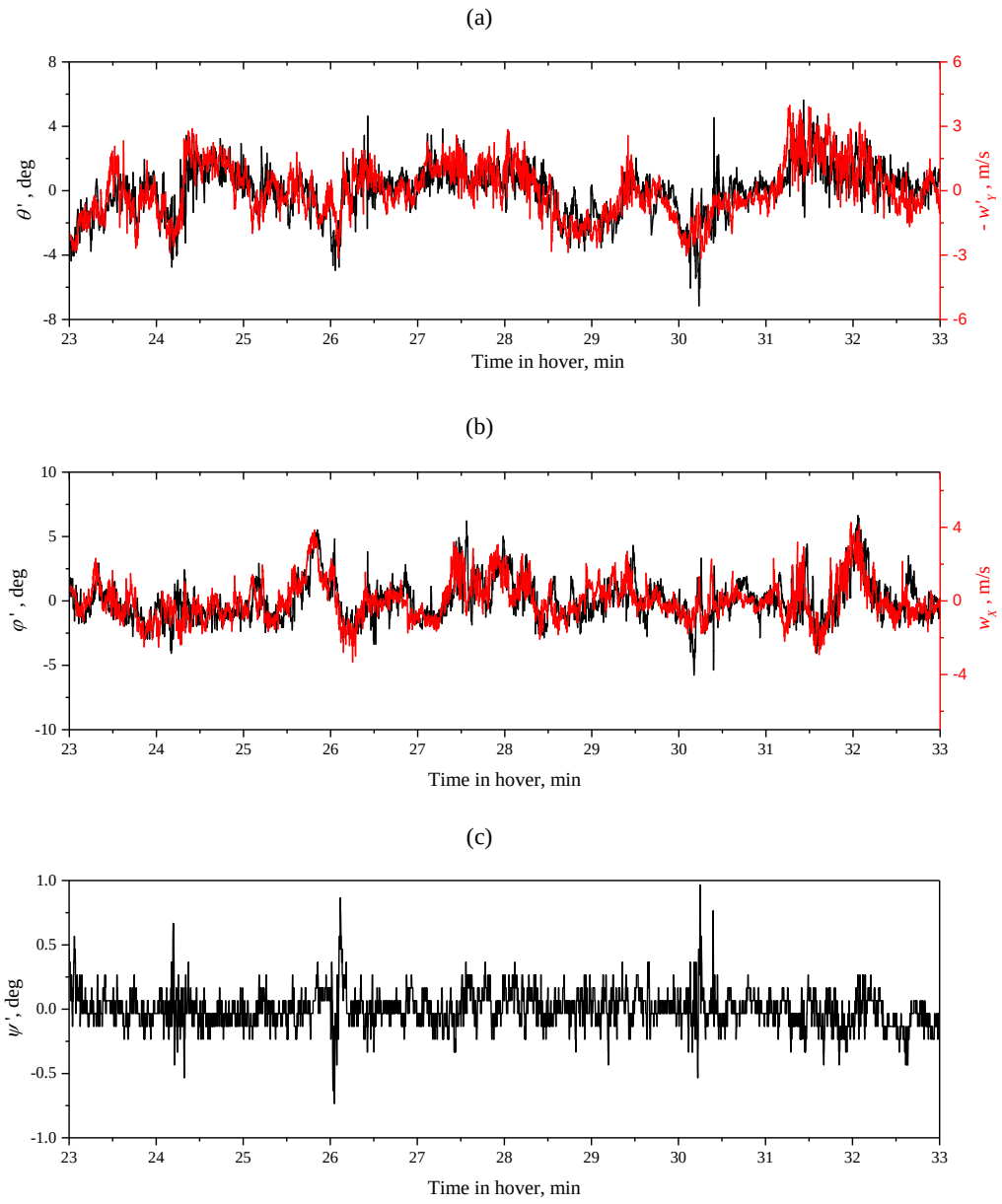

Figure 3. Variations in (a) pitch, (b) roll, and (c) yaw angles (black curve), in the turbulent flow velocity components (a) w_Y and (b) w_X during hovering.

According to the AMK-03 data, anisotropy of the turbulent flow velocity fluctuations was observed during the measurements in the atmosphere: the spectra of fluctuations of the horizontal components coincide, but differ from the spectrum of fluctuations of the vertical components. The comparison of Figs. 4a and 4b shows a similar behavior of fluctuations of the Euler angles: the spectra of fluctuations of the pitch and roll angles coincide, but differ from the spectrum of fluctuations in the yaw angle. Equation (8) implies that the spectral tensor cannot be determined by a single scalar function, which means anisotropy of fluctuations of the wind velocity and Euler angles. Thus, in the altitude holding mode, the spectra of fluctuation of the pitch, roll, and yaw angles are anisotropic if the fluctuations of the turbulent flow velocity in the atmosphere are anisotropic.

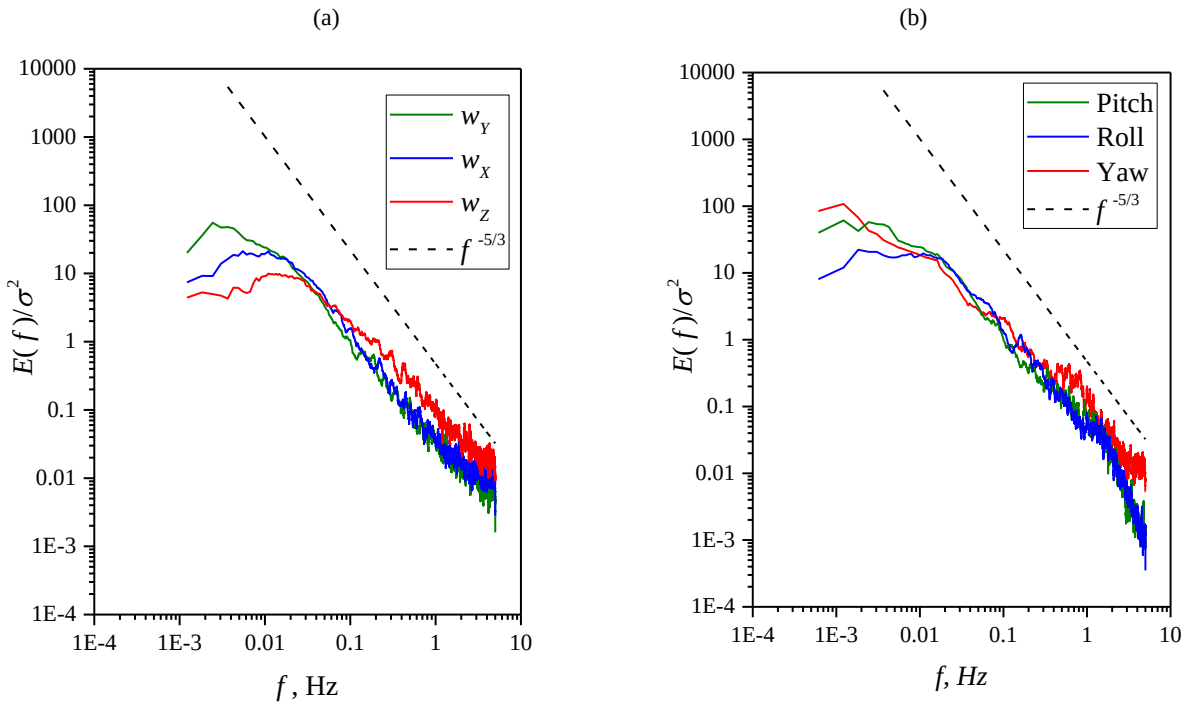

Figure 4. Spectra of fluctuations of (a) turbulent flow velocity and (b) pitch, roll, and yaw angles.

Figure 5 shows the results of comparison between the spectra of fluctuations of the turbulent flow velocity and of the pitch, roll, and yaw angles. The dashed curve in Figure 5 shows the power spectrum of fluctuations $E(f) \sim f^{-5/3}$, which corresponds to the Kolmogorov–Obukhov five-thirds law; σ^2 is the normalization coefficient.

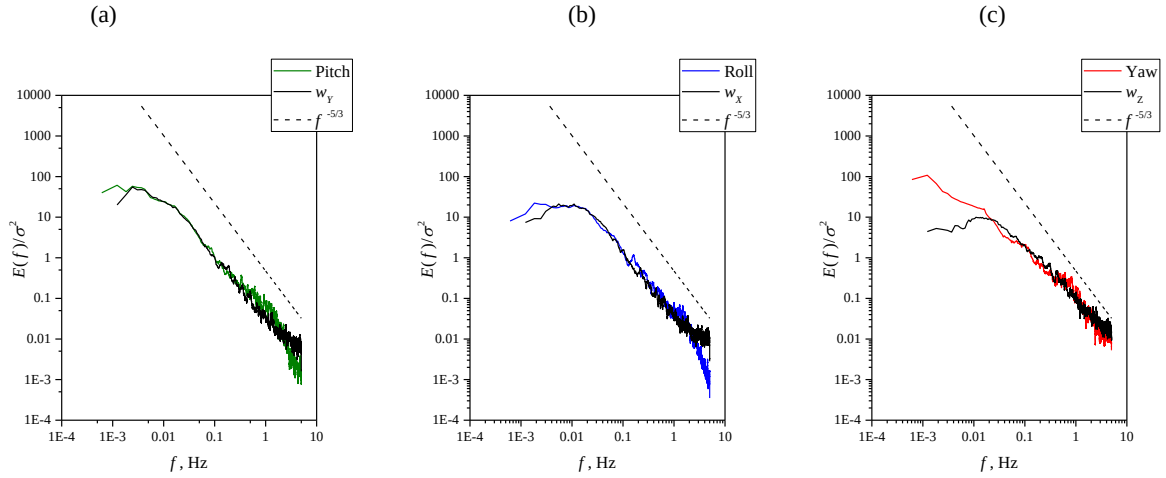

Figure 5. Comparison between the spectra of fluctuations of turbulent flow velocity components and (a) pitch, (b) roll, and (c) yaw angles

Figures 5a and b witness that the spectra of fluctuations of the pitch and roll angles and the spectra of fluctuations of the horizontal wind velocity components are generally general coincide, and significant differences are observed in the high-frequency region of the spectrum. In contrast to fluctuations of the θ' and φ' angles, the spectrum of fluctuations of the yaw angle coincides with that of the vertical wind velocity component in the high-frequency region.

5. ACKNOWLEDGMENTS

Thereported study was funded by RFBR, project number 19-29-06066 mk.

REFERENCES

[1] Cornman, L. B., Chan W. N., "Summary of a Workshop on Integrating Weather into Unmanned Aerial System Traffic Management," Bull. Amer. Meteor. Soc. 98(10), ES257–ES259 (2017). https://doi.org/10.1175/BAMS-D-16-0284.1

[2] Palomaki, R. T., Rose, N. T., van den Bossche, M., Sherman, T. J., and De Wekker, S. F. J., "Wind estimation in the lower atmosphere using multirotor aircraft," J. Atmos. Ocean. Technol. 34, 1183–1190 (2017). DOI: 10.1175/JTECH-D-16-0177.1

[3] Neumann, P. P. and Bartholmai, M., "Real-time wind estimation on a micro unmanned aerial vehicle using its internal measurement unit," Sens. Actuators 235A, 300–310 (2015). DOI:10.1016/j.sna.2015.09.036.

[4] González-Rocha, J., De Wekker, S. F. J., Ross, S. D., and Woolsey, C. A., "Wind Profiling in the lower atmosphere from wind-induced perturbations to multirotor," UAS. Sensors 20, 1341 (2020).

[5] González-Rocha, and Woolsey, C. A., "Cornel Sultan measuring atmospheric winds from quadrotor motion," AIAA Atmospheric Flight Mechanics Conference. 9–13 January 2017, Grapevine, Texas. DOI: 10.2514/6.2017-1189.

[6] Allison, S.; Bai, H.; Jayaraman, B. Wind estimation using quadcopter motion: A machine learning approach. Aerosp. Sci. Technol. **2020**, 98, 105699.

[7] Stull, R.B. [An Introduction to Boundary Layer Meteorology], Kluwer Academic Publishers, Netherlands (1989).

[8] Monin, A. S. And Yaglom, A. M. [Statistical Hydromechanics. Part 2. Turbulent Mechanics], Nauka, Moscow, (1967).